

## ULTRAFAST IN-LINE CAPABLE REGENERATION PROCESS FOR PREVENTING LIGHT INDUCED DEGRADATION OF BORON-DOPED P-TYPE CZ-SILICON PERC SOLAR CELLS

A. A. Brand<sup>1</sup>, K. Krauss<sup>1</sup>, P. Wild<sup>2</sup>, S. Schörner<sup>2</sup>, S. Gutscher<sup>1</sup>, S. Roder<sup>1</sup>, S. Rein<sup>1</sup>, J. Nekarda<sup>1</sup>

<sup>1</sup>Fraunhofer Institute for Solar Energy Systems ISE, Heidenhofstr. 2, 79110 Freiburg, Germany

<sup>2</sup>Rehm Thermal Systems GmbH, Leinenstrasse 7, 89143 Blaubeuren, Germany

Phone: +49 761 - 4588 5053; e-mail: andreas.brand@ise.fraunhofer.de

**ABSTRACT:** Solar cells based on boron-doped p-type Czochralski-grown silicon (Cz-Si) substrates suffer from light-induced degradation (LID) which is related to a metastable boron-oxygen defect and limits the achievable cell efficiency significantly, but can be eliminated by carrier injection at elevated temperatures within a so-called regeneration process. We have developed an ultrafast regeneration process (UFR) to prevent up to 98% of the LID effect in less than 4 seconds process-time. The technology behind this process has been implemented in an in-line prototype tool with belt speeds of up to 8000 mm/min. Compared to competing techniques the technology introduced here enables tools with smaller footprint and broader process window, offering irradiation intensities up to 1 MW/m<sup>2</sup> and temporal and spatial modulation of the irradiation intensity with up to 100 Hz. Undistorted in-situ temperature measurements can be acquired via commercially available thermographic imaging equipment. Further, we introduce a new parameter called regeneration completeness in order to allow benchmarking for BO-regeneration processes. It quantifies the effectiveness of BO-regeneration processes independent of the overall efficiency in order to allow a direct comparison of the quality of different regeneration processes.

**Keywords:** LID, BO-defect, regeneration, stabilization, annealing

### 1 INTRODUCTION

Boron-doped Czochralski-grown silicon (Cz-Si) is widely used as substrate in the photovoltaic industry. However, this material type suffers from a degradation of bulk lifetime within the first hours of light exposure what is known as light-induced degradation (LID) [1]–[8]. The responsible defect is widely known as the boron-oxygen (BO) defect [3].

The efficiency of passivated emitter and rear cells (PERC) [10] can benefit significantly from a higher base doping concentration which reduces the resistive losses in the bulk, allows a reduction of base contact area and, hence, rear-side recombination. However, an increased boron base doping concentration implies a stronger LID effect and, thus, leads to a stronger limitation of bulk lifetime and efficiency, which overcompensates possible gains [4], [11]. Therefore, avoidance or reversal of BO-related LID is one of the most important singular enhancements for state of the art high-efficiency PERC solar cells on boron-doped Cz-Si substrates. As the LID-related efficiency losses typically amount up to 1-2%<sub>abs</sub>, the avoidance or reversal of the LID directly leads to a respective efficiency advantage without any significant changes in technology [12].

Thus, prevention of the BO-related LID is a key enabler for high-efficiency solar cells manufactured from industry-standard boron-doped Cz-Si wafers. Ways to avoid BO-related LID are the replacement of boron with gallium during crystallization [13] or techniques to reduce oxygen concentration in the crystal [3]. Another way to strongly prevent BO-related LID is applying a so-called *regeneration* [14]. When first reported regeneration required several minutes to hours, but recently approaches for fast regeneration processes with industrially feasible process time in the order of seconds have been reported [16], [27], [17]. Within this paper we present the integration for a fast regeneration process and report on its implementation in an industrial tool. With a large number of solar cell manufacturers adopting the PERC solar cell concept [18], the demand for such a regeneration process is bound to increase.

### 2 BO-DEFECT

#### 2.1 BO-defect states

An important characteristic of the BO-defect is that according to a model introduced by Herguth et al. [14] it exhibits three different defect states. In the *annealed state* which is metastable upon illumination or carrier-injection, the BO-defect is inactive and bulk lifetime only limited by other defects. This is the state of the BO-defect after fast firing which is typically the last process in the solar cell production. In the *degraded state*, the bulk lifetime is significantly reduced by BO-defect recombination [4], [19]. This state is stable under light irradiation at room temperature and typically limits the performance of boron-doped Cz-Si solar cells [20]. The third state is often called the *regenerated, passivated or stabilized state*. In this state the BO-defect is deactivated as in the annealed state but in addition stable upon illumination and carrier injection. Note, that incomplete transitions between the states are possible and lifetime can be limited by a mixture of the states and their recombination. The regenerated state is preferred for solar cells since it offers higher bulk lifetime and thus higher solar cell efficiency over a long period of operation.

#### 2.2 BO-defect state transitions

The BO-defect states are metastable and can be converted from one state to another by combinations of charge carrier injection and temperatures. The transition rates between the states depend on both, carrier injection and temperature, see Ref. [Niewelt] and references therein [1], [14]. Different combinations of both change the ratio of these transition rates, so over time an equilibrium of all three defect states forms. Although there will be a combination of states in most cases, we simplify our naming to the dominant state from now on.

Carrier injection can be achieved by applying a forward current to the solar cell or by light illumination. High-intensity light illumination in the range of tens or hundreds of kilowatts per square meter can reach much higher injection levels than forward current through a

solar cell, which would be limited by the series resistance and thus damage or destroy the electrical contacts. Thus, high-intensity illumination is more practical for injecting high charge carrier densities. From here on, we will restrict ourselves to light illumination with photon energies above the silicon bandgap ( $E_{ph} \geq 1.17$  eV) as carrier injection source. Furthermore, we discuss only the open-circuit case when applying carrier injection via light illumination.

The annealed state converts to the degraded state during light illumination at temperatures below 45°C [1], [2], [21]. The full transition from the annealed to the degraded state is in the order of 24 h when light intensities of 1 kW/m<sup>2</sup> are applied [14].

The degraded state can be converted back to the annealed state by annealing in the dark for few minutes at temperatures > 200°C [1].

The degraded state can also be converted to the regenerated state by light illumination at elevated temperatures > 65°C. This process is often called *BO-regeneration* or just *regeneration* [8], [14]. It is known that illumination with higher light intensities increases the transition rate towards the regenerated state [15], [16] but also causes higher process temperatures which in turn increase the transition rate towards the annealed state [2].

### 3 REGENERATION COMPLETENESS

#### 3.1 Complete approach

In order to be able to benchmark and compare different regeneration processes on different solar cells, it is important to have a robust and technology-independent measure for the amount of defects which are transferred to the regenerated state upon the applied treatment. An absolute efficiency gain or loss is not a suitable indicator to assess the regeneration result quantitatively since it depends on the solar cell manufacturing process and absolute efficiency.

In order to ensure comparability of the regeneration results for different regeneration processes, we introduce an easy to understand measure of process effectiveness, called *regeneration completeness RC*, which is defined as

$$RC = \frac{\eta_{\text{regenerated}} - \eta_{\text{degraded}}}{\eta_{\text{annealed}} - \eta_{\text{degraded}}}$$

The *RC* value represents the amount of prevented degradation as a fraction of the total efficiency loss a single solar cell exhibit without any *BO-regeneration*. The *RC* values should be between 0 and 1 and are higher the the more defects have been transferred to the regenerated state. However, if other properties of the solar cell are altered by the regeneration process, the *RC* values could extend beyond the range of 0-1.

Proper *RC* calculations are often hindered by transitions between the metastable defect states of iron, i.e., the formation of interstitial iron ( $Fe_i$ ) upon illumination and the formation of iron-boron pairs ( $FeB$ ) upon dark storage [22]. Thus, the presence of iron associated with boron or as an interstitial defect after each treatment need to be taken into consideration when taking *IV*-measurements at different *BO*-states [3], [22]–[24]. In figure 1 the left column illustrates the experimental plan of temperature and illumination treatments which is

required for the formation and elimination of different defect types as basis for a precise calculation of *RC*. The expected *BO* and  $FeB/Fe_i$  defect states after each process step are listed in the right columns. The procedure is similar to the characterization performed in Ref. [9].

Process steps	defect state	
	BO	FeB
solar cell manufacturing process + delivery	?	$Fe_i$
light illumination ( $I \approx 0.2$ kWm <sup>-2</sup> , $T > 40^\circ\text{C}$ , $t \geq 36$ h)	degraded	$Fe_i$
dark storage ( $T \approx 25^\circ\text{C}$ , $t \geq 24$ h)	degraded	$FeB$
IV measurement $\rightarrow \eta_{\text{degraded}}$	?	?
anneal ( $T \approx 200^\circ\text{C}$ , $t = 20$ min)	annealed	$Fe_i$
dark storage (dark $T \approx 25^\circ\text{C}$ , $t \geq 24$ h)	annealed	$FeB$
IV measurement $\rightarrow \eta_{\text{annealed}}$	?	$FeB$
regeneration process	?	$Fe_i$
light illumination ( $I \approx 0.2$ kWm <sup>-2</sup> , $T > 40^\circ\text{C}$ , $t \geq 36$ h)	?	$Fe_i$
dark storage ( $T \approx 25^\circ\text{C}$ , $t \geq 24$ h)	?	$Fe_i$
IV measurement $\rightarrow \eta_{\text{stable}}$	?	$FeB$

**Figure 1:** Experimental plan for determination of regeneration completeness *RC*, left column. On the right the according defect states of *BO* and  $FeB$  are listed.

First, we degrade the solar cells by a light illumination step using standard fluorescent tube lamps with a light intensity of roughly 200 W/m<sup>2</sup>. During illumination the wafers reach a temperature slightly above 40°C. This light illumination is maintained for at least 36 h in order to ensure complete degradation. After light illumination possible iron defects are fully present as interstitial iron ( $Fe_i$ ) as  $FeB$  pairs have dissociated.. Dark storage of the solar cells at approximately 25°C for at least 24 h causes the iron to pair ( $FeB$ ), the *BO*-defect being still fully active. Subsequently we conduct the first *IV*-measurement which gives  $\eta_{\text{degraded}}$ , the efficiency at full *BO*-related LID but without the influence of  $Fe_i$ .

Next, we apply a thermal anneal at 200°C in the dark for 20 minutes using a hotplate in order to convert the *BO*-defect to its annealed state. It is necessary to do this treatment without any light illumination or other carrier injection to avoid transitions to the regenerated state. This is unwanted at this point since we try to investigate the effectiveness of a different regeneration process. Another dark storage is conducted in order to ensure iron is in the  $FeB$  state. We then conduct a second *IV*-measurement of the solar cells which gives  $\eta_{\text{annealed}}$ , the efficiency of the solar cells without any *BO*-recombination. This state is comparable to the one we expect directly after fast firing, the last processing step of the typical PERC solar cell production.

Now, we apply the regeneration process. After regeneration, the entirety of the *BO*-defects is in an unknown state, which likely is a mixture of the annealed, degraded and regenerated defect state. Due to the light illumination and the high temperatures upon regeneration, iron is in the  $Fe_i$  state. We conduct another light illumination step at room temperature to convert all remaining annealed *BO* defects to the degraded state and then apply another dark storage step to convert iron into the  $FeB$  state (for both steps the same parameters as before are used). Afterwards the solar cells are *IV*-measured a third time which gives  $\eta_{\text{regenerated}}$ .

This concludes the experiment. Inserting the values for all three input values for  $\eta_{\text{degraded}}$ ,  $\eta_{\text{annealed}}$  and

$\eta_{\text{regenerated}}$  gives the RC for each solar cell.

### 3.2 Practical approach for time efficient evaluation

The determination of the actual regeneration completeness of each solar cell as described above requires a time consuming series of dark storage, light illumination, annealing and *IV*-measurements. Therefore, we also define a more time efficient way for evaluation of regeneration results of large sample. The output parameter of the simplified procedure is called *practical regeneration completeness* (*pRC*) to differentiate it from the precise RC value extracted from the full procedure (see Figure 1). Figure 2 illustrates the procedure that is applied for determining *pRC*. Because of its simplicity and increasing robustness with sample size the determining *pRC* is very well suited to evaluate the of different regeneration processes on an industrial scale.

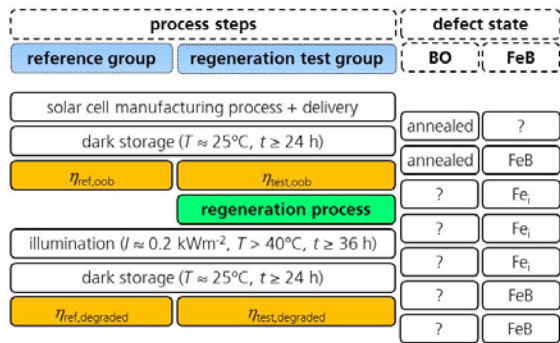


**Figure 2:** Simplified procedure to determine the practical regeneration completeness *pRC*.

After solar cell manufacturing it is assumed that for all the solar cells almost all the BO-defects are in the annealed state which is usually the case if the solar cells have not been exposed to light or forward bias current after fast firing.

Like in section 3.1, a dark storage step is applied before each *IV*-measurement to ensure that possible iron defects are always in the FeB state upon measurement and are thus fully subtracted out in the RC/*pRC* calculation. The first *IV*-measurement represents the out of box (oob) efficiency of each solar cell  $\eta_{\text{oob}}$ . Randomly picking some of the solar cells as a reference group is not very effective as it could generate a non-representative subset. The out of box *IV*-measurements are evaluated in order to generate a small subset of solar cells for the reference group which have a comparable distribution of the *IV* values as the regeneration group.

The reference group is degraded by applying a light illumination step. This is followed by another dark storage step. Finally, the solar cells of the reference group are *IV*-measured again resulting in  $\eta_{\text{ref,degraded}}$ .

The regeneration test group is treated with the regeneration process. It then undergoes the same light illumination and dark storage steps as the reference group to degrade all BO-defects which remain in the annealed state. Finally, *IV*-measurements of the test group are conducted resulting in  $\eta_{\text{test,regenerated}}$ . The *pRC* can now be calculated for each solar cell as follows:

$$pRC = 1 - \frac{\eta_{\text{test,oob}} - \eta_{\text{test,regenerated}}}{\Delta\bar{\eta}_{\text{ref}}}$$

With  $\Delta\bar{\eta}_{\text{ref}}$  representing the average efficiency difference

for all *n* solar cells of the reference group between out of box and degraded *IV*-measurements.

## 4 ULTRAFAST REGENERATION TECHNOLOGY

There are some industrial tools available today that use high-intensity lamps or LEDs for BO-regeneration. Laser radiation can deliver much higher intensities. It has been shown by the authors of this paper [17] and other groups [15], [16], [25] that using laser irradiation intensities of several tens to hundreds of kilowatt per square meter can speed up the full regeneration of Cz-Si wafers to as little as 0.2 seconds. However, we are unaware of anyone having developed a laser-based production tool for regeneration at this point. Because of the very fast regeneration that is being enabled by this drastic intensity increase we refer to this regeneration technology ultrafast regeneration (UFR).

Our regeneration technology offers several advantages for inline BO-regeneration systems compared to other technologies used in industrially implemented tools. Some notable advantages are:

- laser irradiation intensities of up to 1 MW/m<sup>2</sup>
- small footprint tooling
- maximum carrier injection per generated heat
- simple in-situ temperature measurement
- durable illumination components

We use laser radiation sources which offer significantly higher irradiation intensity up to 1 MW/m<sup>2</sup> and higher compared to competing light sources like lamps and LEDs. Figure 3 illustrates intensities for different irradiation sources in a regeneration tooling setup.

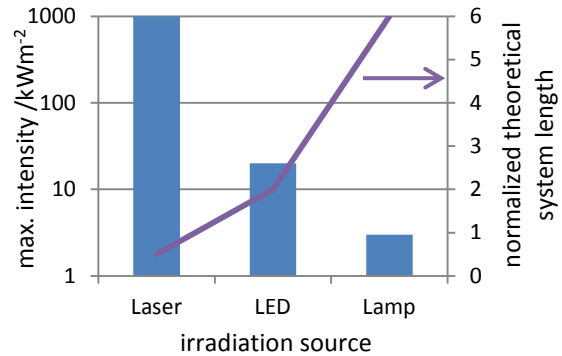


**Figure 3:** Comparison of the irradiation intensity for different light sources and the theoretical lengths for inline systems depending on the intensity. An in-line belt speed of 6000 mm/min is assumed.

Because of the higher available irradiation intensity, an UFR in-line production tool can be of much smaller footprint while maintaining the same or higher wafer throughput compared to in-line tools based on other light sources. Figure 3 also displays the estimated system lengths achieving the same degree of regeneration completeness for different irradiation sources. The system lengths for laser is estimated taking into account experimental values for regeneration times in dependence

of irradiation intensities  $< 1 \text{ MW/m}^2$  and under the assumption of 6000 mm/min belt transportation speed. The system lengths for the LED and Lamp as irradiation source are estimated taking into account publically available information about processing speeds from manufacturers of regeneration tools. The estimation reveals that an UFR regeneration system can probably be built with less than half the length of a system based on high power LEDs.

One of the key problems to adopt high-intensity light sources of any kind for the BO-regeneration process is the heat accumulation which can cause the wafers to become hotter than reasonable for the optimal process window. The heat generated in the solar cells by photon absorption correlates with the intensity. Therefore, it is our goal to maximize the minority charge carrier density in the solar cell while minimizing the temperature. UFR uses photon energies of 1.27 eV which add only 0.1 eV of excessive energy per excited electron since the bandgap of silicon is 1.17 eV. With silicon being an indirect semiconductor using irradiation with 1.17 eV photon energy would not be ideal since a major part of the photonic flux would be transmitted to the rear side of the solar cell where the photons would only add to the heat but not the carrier injection in the silicon.

Controlling the solar cell temperature during the regeneration process is of great importance to the regeneration effectiveness, as mentioned above [14], [26]. Figure 4 shows an example of an in situ temperature measurement during the UFR process. The image was acquired using a standard M-IR camera in a spectral range of 7.5–13  $\mu\text{m}$ . The emissivity is calibrated for the area in between busbars.

Such thermographic imaging is easily implemented since the laser radiation used for the UFR process has a bandwidth of less than  $\pm 10 \text{ nm}$  and no background emissions in the spectrum of the camera. This is a key advantage compared to competing light sources.

The laser components we use for UFR are proven to be highly reliable and maintenance free under 24/7 production scenarios. A continuous test by the manufacturer at 100% output power over  $> 19000 \text{ h}$  operation did result in a less than 2% deviation in irradiation intensity.

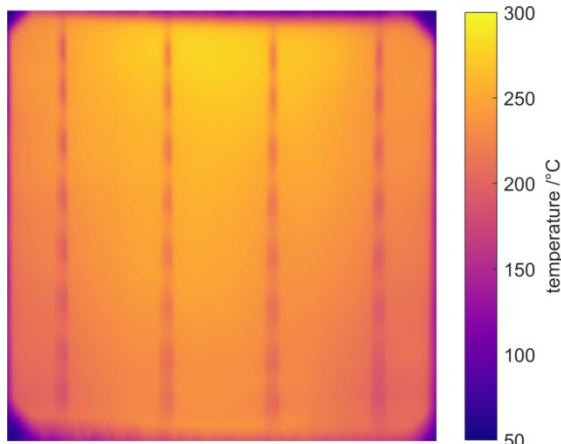


**Figure 4:** In-line measurement of the temperature of a solar cell along the laser irradiation path. This image is recorded by a commercial infrared camera.

## 5 LABORATORY SCALE PROCESS

The development of UFR technology was based on a lab-scale tool before integration into an industrial production prototype.

We use industry standard p-type PERC solar cells based on Cz-Si wafers which we obtained from a renowned solar cell manufacturer. The rear side passivation of the solar cells is passivated with an  $\text{AlO}_x/\text{SiN}_x$  PECVD passivation stack. The rear contacts are realized using laser contact opening (LCO) of the rear side passivation and screen printing of aluminium paste. The front contacts consist of screen-printed silver paste. The contact formation is realized by a fast firing process.

Process variations have been performed on a UFR prototype in order to optimize the achieved *pRC*, which is determined as described in figure 2. The best UFR process achieves 98% *pRC* with an irradiation length of less than 4 seconds.

In order to test the robustness of the UFR process we apply the optimized process parameters from the above mentioned experiment to PERC solar cells from four additional solar cell manufacturers, all using boron-doped Cz-Si. The solar cells from these manufacturers may exhibit differences in boron and oxygen concentration. The different manufacturers are also likely to use different production technologies and processing routes all of which are known to have a strong influence on the results of a regeneration process.

The results are illustrated in figure 5. Manufacturer #1 represents the same kind of solar cells which were used for the process optimization with *pRC* = 98%.

The regeneration completeness for manufacturers #2-5 show an average *pRC* of 82.1%. This result illustrates that the UFR process can be very effective at regenerating standard mass produced Cz-Si PERC solar cells even without manufacturer-specific optimization. However, optimization seems obvious when integrating any regeneration processes into a production line and, hence, the need for a tool which can offer this flexibility.

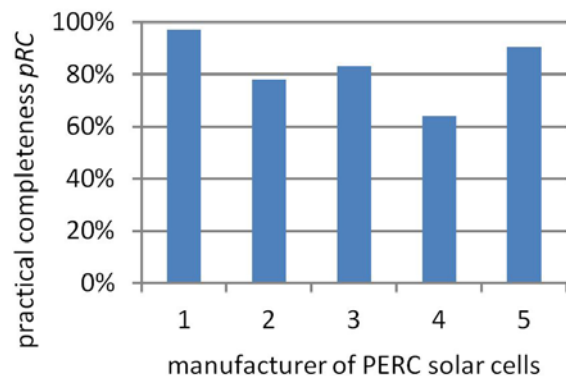


**Figure 5:** Example for regeneration completeness of an UFR process for solar cells of different manufacturers. These results were achieved using a non-inline laboratory setup. The process parameters applied to all groups are the ones optimized for manufacturer #1.

Since our UFR technology offers a wide parameter space, we have observed that simple process optimization for the other manufacturers yields similarly good results as the *pRC* = 98% from manufacturer #1.

## 6 IN-LINE TOOL

We have developed a prototype UFR system for solar cell production. Figure 6 shows the completed UFR system with an overall footprint of less than 4 m<sup>2</sup>. Due to the compactness, this tool can be easily integrated into new as well as existing production sites.

This system demonstrates the production-readiness of the UFR technology including an integrated inline temperature control of the solar cells during laser irradiation.

In a first UFR experiment using the recently completed inline tool we achieved a preliminary result of  $pRC = 86\%$  at a belt speed of 6 m/min. This value was achieved on solar cells of manufacturer #1, described in section 5.1. The result demonstrates the successful implementation of our UFR technology into a production tool. Other regeneration tools on the market claim to achieve similar levels of LID-prevention although it is unknown to the authors of this article how these are determined.



**Figure 6:** Prototype of single track inline regeneration tool based on UFR technology. It offers a belt speed of up to 8000 mm/min and a footprint of less than 4 m<sup>2</sup>.

## 7 CONCLUSION & OUTLOOK

We have introduced a new measurement parameter called *regeneration completeness (RC)* which quantifies the effectiveness of BO-regeneration processes independently of overall solar cell efficiency. Furthermore, a more time efficient procedure for large sample sets which results in the *practical regeneration completeness (pRC)* has been introduced. This allows for the first time to easily compare the process effectiveness of different regeneration processes on an industrial scale instead of comparing absolute efficiency differences on a very limited number of solar cells.

A technology for ultrafast regeneration to reduce boron-oxygen related light-induced degradation of p-type Czochralski-grown silicon solar cells has been developed. The UFR process has been demonstrated to achieve up to 98% regeneration completeness in < 4 s irradiation time. The ability to monitor and control intensity and temperature distribution during the process allows accurate control of processing parameters and, thus, enables more options for process optimizations to accommodate for differences in the solar cell

manufacturing process.

We have implemented this technology in an in-line production tool with industrial belt speeds up to 10 m/min and we have achieved up to 86% practical regeneration completeness in our preliminary tests. To our knowledge, this is the fastest in-line LID prevention process available for manufacturing.

## 8 ACKNOWLEDGEMENTS

The authors would like to thank their colleagues at the Fraunhofer institute for solar energy systems (ISE) for their help with regeneration experiments and solar cell characterization. This work was funded by the German Federal Ministry for Economic Affairs and Energy within the research project “UFO” under contract number 0324080.

## 9 REFERENCES

- [1] H. Fischer and W. Pschunder, “Investigation of photon and thermal induced changes in silicon solar cells,” in *Photovoltaic Specialists Conference, 10 th, Palo Alto, Calif, 1974*, pp. 404–411.
- [2] S. Glunz, S. Rein, W. Warta, J. Knobloch, and W. Wettling, “On the degradation of Cz-silicon solar cells,” in *Proc. 2nd WC PVSEC, 1998*.
- [3] S. Rein, S. Diez, R. Falster, and S. Glunz, “Quantitative correlation of the metastable defect in Cz-silicon with different impurities,” in *Photovoltaic Energy Conversion, 2003. Proceedings of 3rd World Conference on, 2003*, vol. 2, pp. 1048–1052.
- [4] K. Bothe, R. Sinton, and J. Schmidt, “Fundamental boron-oxygen-related carrier lifetime limit in mono- and multicrystalline silicon,” *Prog. Photovolt. Res. Appl.*, vol. 13, no. 4, pp. 287–296, Jun. 2005.
- [5] B. Lim, “Boron-oxygen-related defects in crystalline silicon: Formation, recovery kinetics, and impact of compensation,” Südwestdeutscher Verlag für Hochschulschriften, Saarbrücken, 2012.
- [6] T. U. Naerland, “Characterization of light induced degradation in crystalline silicon,” Univ. Sci. Technol., Trondheim, Norway, Saarbrücken, 2013.
- [7] J. Lindroos and H. Savin, “Review of light-induced degradation in crystalline silicon solar cells,” *Sol. Energy Mater. Sol. Cells*, vol. 147, pp. 115–126, Apr. 2016.
- [8] T. Niewelt, J. Schon, W. Warta, S. W. Glunz, and M. C. Schubert, “Degradation of Crystalline Silicon Due to Boron–Oxygen Defects,” *IEEE J. Photovolt.*, vol. 7, no. 1, pp. 383–398, Jan. 2017.
- [9] F. Fertig, K. Krauß, and S. Rein, “Light-induced degradation of PECVD aluminium oxide passivated silicon solar cells: Light-induced degradation of PECVD aluminium oxide passivated silicon solar cells,” *Phys. Status Solidi RRL - Rapid Res. Lett.*, vol. 9, no. 1, pp. 41–46, Jan. 2015.
- [10] A. W. Blakers, A. Wang, A. M. Milne, J. Zhao, and M. A. Green, “22.8% efficient silicon solar

- cell,” *Appl. Phys. Lett.*, vol. 55, no. 13, pp. 1363–1365, Sep. 1989.
- [11] S. Rein, W. Warta, and S. Glunz, “Investigation of carrier lifetime in p-type Cz-silicon: specific limitations and realistic prediction of cell performance,” in *Photovoltaic Specialists Conference, 2000. Conference Record of the Twenty-Eighth IEEE*, 2000, pp. 57–60.
- [12] S. Wasmer, A. A. Brand, and J. Greulich, “Metamodeling of numerical device simulations to rapidly create efficiency optimization roadmaps of monocrystalline silicon PERC cells,” *Energy Procedia*, 2017.
- [13] S. Glunz, S. Rein, J. Knobloch, W. Wettling, and T. Abe, “Comparison of boron- and gallium-doped p-type Czochralski silicon for photovoltaic application,” *Prog. Photovolt. Res. Appl.*, vol. 7, no. 6, pp. 463–469, 1999.
- [14] A. Herguth, G. Schubert, M. Kaes, and G. Hahn, “Avoiding boron-oxygen related degradation in highly boron doped Cz silicon,” in *Proceedings of the 21st European Photovoltaic Solar Energy Conference*, 2006, pp. 530–537.
- [15] P. Hamer, B. Hallam, M. Abbott, and S. Wenham, “Accelerated formation of the boron-oxygen complex in p-type Czochralski silicon: Accelerated formation of the boron-oxygen complex in p-type Czochralski silicon,” *Phys. Status Solidi RRL - Rapid Res. Lett.*, vol. 9, no. 5, pp. 297–300, May 2015.
- [16] S. Wilking, J. Engelhardt, S. Ebert, A. Herguth, and G. Hahn, “High speed regeneration of BO-defects: Improving long-term solar cell performance within seconds,” presented at the EUPVSEC, Amsterdam, 2014.
- [17] A. A. Brand, S. Wasmer, M. Graf, J.-F. Nékarda, and R. Preu, “Laser based evolution of the PERC process chain,” presented at the PVCellTech, Kuala Lumpur, 2016.
- [18] “International Technology Roadmap for Photovoltaic (ITRPV) 2017,” *International Technology Roadmap for Photovoltaic (ITRPV)*. [Online]. Available: <http://www.itrpv.net/>. [Accessed: 17-Sep-2017].
- [19] S. Rein, W. Warta, and S. W. Glunz, “Investigation of carrier lifetime in p-type Cz-silicon: specific limitations and realistic prediction of cell performance,” *Proceedings of the 28th IEEE Photovoltaic Specialists Conference*, Anchorage, USA, pp. 57–60, 2000..
- [20] J. Schmidt *et al.*, “Impurity-related limitations of next-generation industrial silicon solar cells,” *IEEE J Photovolt.*, vol. 3, pp. 114–118, 2013.
- [21] J. Schmidt, A. G. Aberle, and R. Hezel, “Investigation of carrier lifetime instabilities in Cz-grown silicon,” in *Conference Record of the Twenty Sixth IEEE Photovoltaic Specialists Conference - 1997*, 1997, pp. 13–18.
- [22] L. J. Geerligs and D. Macdonald, “Dynamics of light-induced FeB pair dissociation in crystalline silicon,” *Appl. Phys. Lett.*, vol. 85, no. 22, pp. 5227–5229, 2004.
- [23] J. Schmidt and K. Bothe, “Structure and transformation of the metastable boron-and oxygen-related defect center in crystalline silicon,” *Phys. Rev. B*, vol. 69, no. 2, p. 024107, 2004.
- [24] S. Rein and S. W. Glunz, “Electronic properties of interstitial iron and iron-boron pairs determined by means of advanced lifetime spectroscopy,” *J. Appl. Phys.*, vol. 98, no. 11, p. 113711, 2005.
- [25] L. Song *et al.*, “Laser Enhanced Hydrogen Passivation of Silicon Wafers,” *Int. J. Photoenergy*, vol. 501, p. 193892, 2015.
- [26] S. Wilking, C. Beckh, S. Ebert, A. Herguth, and G. Hahn, “Influence of bound hydrogen states on BO-regeneration kinetics and consequences for high-speed regeneration processes,” *Sol. Energy Mater. Sol. Cells*, vol. 131, pp. 2–8, Dec. 2014.
- [27] B. J. Hallam *et al.*, “Advanced hydrogenation of dislocation clusters and boron-oxygen defects in silicon solar cells,” *Energy Procedia*, vol. 77, pp. 799–809, 2015.